

Killing the Hofstadter butterfly, one bond at a time

Adhip Agarwala

Centre for Condensed Matter Theory, Department of Physics, Indian Institute of Science, Bangalore 560 012, India e-mail: adhip@physics.iisc.ernet.in

the date of receipt and acceptance should be inserted later

Abstract. Electronic bands in a square lattice when subjected to a perpendicular magnetic field form the Hofstadter butterfly pattern. We study the evolution of this pattern as a function of bond percolation disorder (removal or dilution of lattice bonds). With increasing concentration of the bonds removed, the butterfly pattern gets smoothly decimated. However, in this process of decimation, bands develop interesting characteristics and features. For example, in the high disorder limit, some butterfly-like pattern still persists even as most of the states are localized. We also analyze, in the low disorder limit, the effect of percolation on wavefunctions (using inverse participation ratios) and on band gaps in the spectrum. We explain and provide the reasons behind many of the key features in our results by analyzing small clusters and finite size rings. Furthermore, we study the effect of bond dilution on transverse conductivity (σ_{xy}). We show that starting from the clean limit, increasing disorder reduces σ_{xy} to zero, even though the strength of percolation is smaller than the classical percolation threshold. This shows that the system undergoes a direct transition from a integer quantum Hall state to a localized Anderson insulator beyond a critical value of bond dilution. We further find that the energy bands close to the band edge are more stable to disorder than at the band center. To arrive at these results we use the coupling matrix approach to calculate Chern numbers for disordered systems. We point out the relevance of these results to signatures in magneto-oscillations.

1 Introduction

Understanding the role of disorder on electronic conduction has been a central theme in all of condensed matter physics [1–4]. Apart from being fundamentally interesting from a theoretical perspective, these problems hold immense significance as they directly bring out (or hide) novel physics in various experimental systems [5]. A major milestone in this pursuit has been the scaling theory of localization which stated that any infinitesimal amount of disorder will inhibit any conductivity in a thermodynamically large $2D$ system [6, 26]. However, a comprehensive understanding of transport in $2D$ is far from complete – two dimensional systems continue to spring surprises with various phenomena, where mesoscopic physics, interactions, disorder and topology interplay [7–10].

One of the essential probes in condensed matter is the magnetic field. Effects of which on a $2D$ electron gas leads to integer and fractional Hall effect [7, 11]. The same phenomena on an idealized square lattice leads to the Hofstadter model [12]. Interestingly this physics has now been realized both in cold-atomic systems [13, 14] and material systems [15, 16]. These systems also possess non-trivial topology and their signatures in transport [17, 18]. Not surprisingly, the effect of disorder on quantum Hall physics has received its due attention [19–22]. For the continuum model – this question can be posed in two ways – how does the conductance change when, while keeping the magnetic

field same, the disorder is increased or; keeping the disorder same, the magnetic field is reduced. The evolution of the Landau levels, in a $2D$ electron gas, and in the lattice setting with a weakening magnetic field has been a matter of debate [23, 24]. For a recent review refer to [25]. It was earlier suggested that to be consistent with the scaling hypothesis [26], the Landau levels will float up to higher energies with decreasing magnetic field or increasing disorder [27–29]. However some numerical calculations have hinted otherwise and have instead suggested that the system undergoes a Chern insulator to normal insulator transition as a function of the strength of the disorder [30]. A two parameter scaling theory has been suggested to understand this transition and a phase diagram was also proposed [31–33].

However disorder comes in various varieties – Anderson disorder [6] is the most famous of them all. In this, random onsite potentials are added to each site of the lattice. The other more stronger kind of disorders are the percolation disorders. They come in two varieties – site and bond. In the former, one randomly removes the sites from the lattice, in the latter, bonds. Till date, quantum site and bond percolation in $2D$ even in absence of a magnetic field is poorly understood and highly debated – the central question being – whether the physics here is different from Anderson disorder [34, 35]. In fact delocalization-localization transition has been predicted in $2D$ for site-dilution on square lattices [36–39]. In this work we limit ourselves to

the discussion on bond percolation. If we define p_b as the probability of a link being present between two neighbouring sites, then in classical bond percolation, percolation threshold occurs at $p_c = 1, 0.5$ and 0.2488 for hyper-cubic lattices in dimensions (D)=1, 2 and 3 respectively [40, 41]. This threshold signifies the point below which there exists no geometrical connecting path between two sides of a lattice. One expects quantum bond percolation threshold p_q to be $> p_c$ since interference effects will tend to further localize the system even if classically a path may exist. Notice that unlike Anderson disorder here exists a natural bound on p_q due to presence of p_c . While finite size scaling analysis shows an existence of a percolation threshold p_q in $3D$ [42], results for $2D$ are still not settled [35]. Some of the previous works have predicted non-zero conductance for $p > p_c$ while others have predicted that all states get localized even for infinitesimal disorder [42–46]. A study of transport in bond percolating system and its comparison with classical Drude theory expectations have also been performed [47]. Recently, bond (and site) percolation on a honeycomb lattice has received major attention in order to understand the nature of divergence of density of states at $E = 0$ [48–51].

As far as the effect of magnetic field is concerned, most of the studies above [30, 32, 33] has been performed for diagonal Anderson disorder. A study of banded off-diagonal disorder was performed in [52]. However the role of percolation disorder on the Hofstadter model has been little investigated. A periodic dependence of p_q was found as a function of magnetic flux in $3D$ while that in $2D$ was also conjectured [53]. Since for bond percolation disorder the exact value of p_q itself is an open question, it is of particular interest to find if there exists a metal insulator transition before we cross the classical percolation threshold in presence of a magnetic field.

In this paper, our motivation is two fold. The first part involves understanding the effect of bond percolation disorder on the Hofstadter butterfly pattern as a function of p_b . We study the model in both high and low concentration of bond dilutions. We find that even at high amount of bond dilution, we have butterfly-like patterns present in the system. We also look at the effect of bond dilution on band gaps and wavefunctions of the system. We provide understanding of the key features of our results from analyzing small clusters and finite size rings. This provides some physical reasoning behind the results and also contrast them from the case of Anderson disorder. The second part involves calculation of the transport quantities (σ_{xy}), where a numerical study based on calculation of Chern numbers is performed using coupling matrix approach [54]. We study the effect of bond percolation disorder on Hofstadter bands and show that there indeed is a metal insulator transition with decreasing p_b for $p_b > p_c$. We also find that the Chern bands close to the band edges are more stable to disorder than the ones close to band center, which means that it takes higher disorder strength for achieving metal to insulator transition at the edge of the band than at the center. This result in

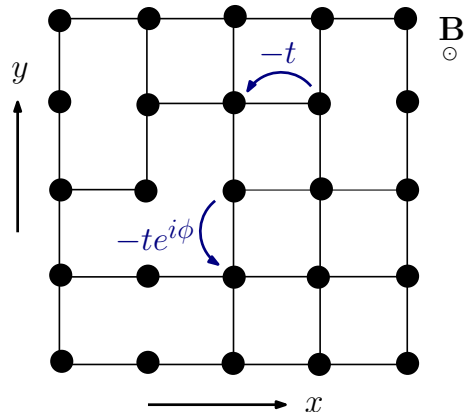


Fig. 1. (Color online) A schematic of a square lattice with some of the bonds removed. p_b is the probability that a bond is present. Therefore, at $p_b = 1$ we have an ideal square lattice. t is the hopping amplitude which is set to 1. ϕ is the Pierls phase which includes the effect of the magnetic field \mathbf{B} .

the low-disorder limit is consistent with the findings for the Anderson disorder case [30].

We now present the plan of the manuscript. In the next section (2) we provide a brief review of the Hofstadter model and present some of the results for finite rings in presence of magnetic field. These will be used later in our study. In the same section we also introduce the percolation problem. Section. 3 contains our results and related discussions on the effect of bond percolation disorder on the Hofstadter butterfly. Here we also discuss the effect of bond dilution on band gaps and on wavefunctions using inverse participation ratios (IPRs). Section 4 contains the essential details about the coupling matrix approach to calculate the Chern number in the presence of disorder and the corresponding results and discussions. In section 5 we summarize our results and speculate some future directions.

2 Formulation and Prelude

2.1 Hamiltonian

The Hamiltonian of our interest is,

$$\mathcal{H} = \sum_{\langle i, j \rangle} -te^{i\phi_{ij}} c_i^\dagger c_j + h.c. \quad (1)$$

where c_i^\dagger, c_j are the creation and annihilation operators for the electrons at site i and j respectively (see Fig.1). The $\langle i, j \rangle$ signifies that the sum is over the nearest neighbors on a square lattice. ϕ_{ij} is the Pierls phase which takes into account the effect of a perpendicular magnetic field \mathbf{B} on the lattice and is given by

$$\phi_{ij} = \frac{e}{\hbar} \int_{\mathbf{r}_j}^{\mathbf{r}_i} \mathbf{A} \cdot d\mathbf{r}, \quad (2)$$

where \mathbf{A} is the corresponding vector potential. t is the hopping integral and is set to 1. $\mathbf{r}_{i(j)}$ denotes the position coordinates of site $i(j)$. We work in Landau gauge

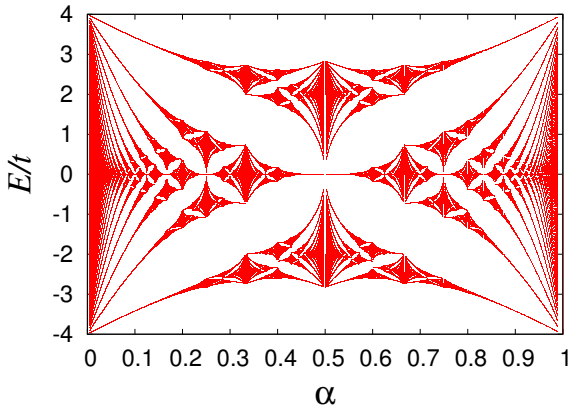


Fig. 2. (Color online) The plot of the energy dispersion as a function of the magnetic flux α . This is the Hofstadter butterfly as was originally reported by Hofstadter [12].

where $\mathbf{A} = (0, Bx, 0)$. This conveniently allows for complex phases only in the hoppings in the vertical direction. The flux per plaquette is given by α in units of h/e . We will ignore the spin of the fermions.

2.2 Hofstadter butterfly

In the gauge we are using, the system has a translational symmetry in y direction – therefore k_y is a good quantum number. For a generic α , the system does not have translational symmetry in x direction. However, when $\alpha = p/q$, where p, q are integers, the problem can be mapped to a reduced Brillouin zone. The eigenvalues can be plotted as a function of α and this leads to the famous Hofstadter butterfly pattern. This self-similar, fractal pattern was first obtained by Hofstadter [12], and is reproduced in Fig. 2.

2.3 Polygon in a magnetic field

Next, let us consider a N sided polygon in a magnetic field. The eigenvalues indexed by M are given by,

$$E_N(M, \alpha_p) = -2t \cos\left(\frac{2\pi}{N}(M + \alpha_p)\right) \quad (3)$$

where $M = \{0, 1, \dots, N-1\}$ and α_p is the flux going through the polygon [55]. Note that α_p is different from the flux per unit plaquette α as introduced in the previous subsection. Fig. 3 shows the dispersion for few representative finite size rings in presence of uniform magnetic field. As can be seen from Fig. 3(c) and (d), both the polygons have 8 sides, but the total flux inside the loops are different. While (c) has $\alpha_p = 3\alpha$, the latter (d) has $\alpha_p = 4\alpha$. These lead to different dispersions ((g)-(h)). These as we will see later will be useful in understanding the results in presence of percolation later.

2.4 Disorder and Percolation

Next we define what we precisely mean by percolating the lattice. p_b is defined as the probability of a link being present between two neighboring sites. This implies that at $p_b = 1$ we have an ideal square lattice. For any value of $p_b < 1$ some of the bonds are removed from the lattice (see Fig.1). For a square lattice there is a classical percolation threshold at $p_b^c \equiv p_c = \frac{1}{2}$. At any value of $p_b < p_c$ there does not exist a classical geometrical path connecting the two sides of the square lattice [35]. Percolation transitions have their own universality classes and distinct critical exponents [41]. Percolation is therefore, a special kind of disorder. Even in quantum transport, note that each bond removal is of the energy scale t which is of the same order as the band-width. However density of bonds removed, quantified as $(1 - p_b)$, is considered as the tuning parameter of disorder strength.

Another kind of percolation problem is the site percolation problem. Here sites are randomly removed from a lattice. We state that although, both bond and site percolation problems retain the sublattice symmetry, the bond problem has some ‘nicer’ features than the site percolation. Once a site is removed from a lattice, it effectively reduces the Hilbert space of the problem. Given an imbalance between the number of sites belonging to the two sublattices, one finds *zero* energy modes in the system, which need to be removed ‘by-hand’ to keep track of non-trivial zero modes [48, 56]. On the contrary, removing bonds on the lattice keeps the dimension of Hilbert space same and only modifies the connectivity between the sites.

As was mentioned in the introductory section, the most well studied disorder problem is the Anderson disorder [6]. Here onsite potentials to each site is chosen randomly from a distribution (mostly ‘box’) between $[-\frac{W}{t}, \frac{W}{t}]$. Thus W is the parameter characterizing the strength of disorder. A review of numerical results on this can be found in [57].

3 Killing the Butterfly

In Fig. 4 the evolution of the Hofstadter butterfly as function of p_b for some representative values of p_b is shown. While $1 - p_b$ can be considered as the ‘strength’ of disorder (like W in Anderson disorder case) we will see that both these disorders are quite different in high disorder limit. Let us first look at the case when p_b is very small and $p_b \ll p_c$ (high disorder limit).

3.0.1 $p_b \ll p_c$

In this limit, the system is below the classical percolation threshold and therefore the lattice has already geometrically broken up into disconnected fragments. As can be seen from Fig.4 (j) and (l) one finds that there are many bands which do not disperse with α . This can be understood from the fact that most of these structures do not have closed loops which have any magnetic flux passing through.

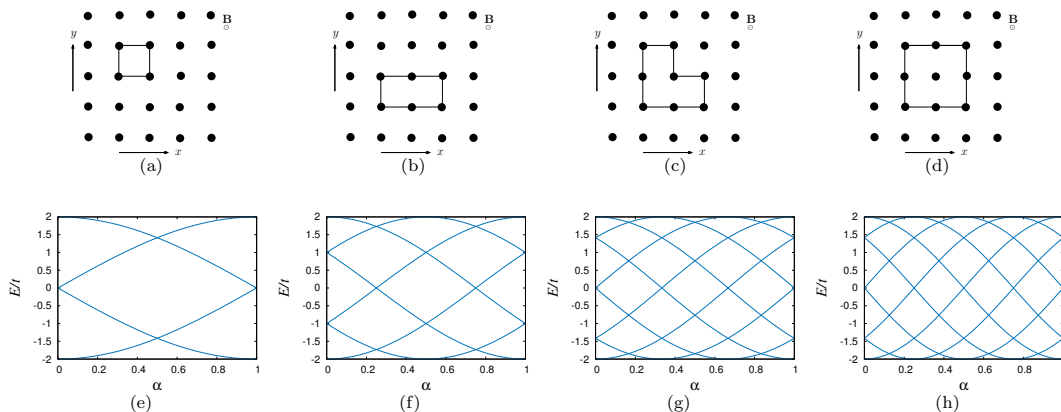


Fig. 3. (Color online) (a) A connected square with a unit flux α per plaquette has a dispersion shown in (e). (b) A polygon with 6 sides, has two unit squares inside, this corresponds to $\alpha_p = 2\alpha$ in eqn. (3) and has a dispersion in (f). A 8-sided polygon can have $\alpha_p = 3\alpha$ (shown in (c)) and $\alpha_p = 4\alpha$ as shown in (d). The corresponding dispersions are shown in (g) and (h) respectively.

We also see that the energies cluster around specific values. To understand these, consider a single site ($j = 1$) connected to N ($j = 2, \dots, N + 1$) other sites with an equal hopping strength $-t$ and no other site is connected to any other. Let the eigenvalues be ε_i , where ($i \in 1, \dots, N + 1$). For a generic N , one finds only two non-zero eigenvalues given by $\pm\sqrt{N}t$. The corresponding eigenvectors are $\frac{1}{\sqrt{2}}(\mp 1, \underbrace{\frac{1}{\sqrt{N}}, \dots, \frac{1}{\sqrt{N}}}_N)^T$. The other

eigenvectors corresponding to zero eigenvalues are of the form $\frac{1}{\sqrt{2}}(0, 0, \dots, \underbrace{1}_i, \dots, \underbrace{-1}_j, \dots, 0)^T$, where i, j denotes the

site index and take the values $\in (2, \dots, N + 1)$ and therefore has $N - 1$ solutions. Since the maximum coordination number for a square lattice problem is 4, the corresponding non-zero eigenvalues are $\pm t(N = 1)$, $\pm\sqrt{2}t(N = 2)$, $\pm\sqrt{3}t(N = 3)$ and $\pm 2t(N = 4)$. Note that all of these structure have no loops and therefore, the eigen-energies will not change with α . Therefore at low p_b limit, as shown in Fig. 4(1), the system has no closed loops and breaks into disconnected fragments. The probability of these structures appearing are $\propto p_b^N$ [41]. This therefore also implies that in this limit we have segregation of eigenvalues at some set of discrete energies and DOS peaks only at these specific energy eigenvalues.

Note that this limit of the Hofstadter model in presence of bond percolation is absolutely distinct from Anderson disorder. The connectivity of each lattice point to the other is not changed in the case of Anderson disorder, and therefore at no value of W do we expect non-dispersing eigenvalues (with α). Similarly, increase in W will never lead the eigenvalues to segregate at select eigenvalues. On the other hand, in bond percolation, at $p_b = 0$ the DOS will show a δ function peak at $E = 0$. However, these states are distinct from the weak disorder $E = 0$ states as also discussed in [58], but rather strongly localized states on individual sites which have very high IPR as will be discussed in detail later.

3.0.2 $p_b < p_c$

As p_b is slightly increased, as can be seen in Fig. 4 (j) and (h), dispersing bands appear. While the complete lattice still does-not have a spanning cluster, what is clear is that we have states in the system which disperse with magnetic flux α . These are due to small clusters which contain closed loops. Take for example the representative plot shown in Fig. 4 (j) and compare the dispersing curve with the Fig. 3 (e). As can be clearly seen they are exactly the same. Therefore, the low p_b ‘‘Hofstadter butterfly’’ will be dominated only by these finite size small loops, as shown in Fig. 3. These have implications for oscillations in magnetization which we will discuss in more detail later. Note that all these states cannot contribute to transport since they reside only on small clusters.

3.0.3 $p_b = 1$

We now discuss the other limit i.e. the clean system. Clearly, even the finite Hofstadter butterfly as shown in Fig. 4(b) has some semblance to the infinite Hofstadter butterfly as shown in Fig. 2, increasing lattice size makes this similarity more and more apparent [55]. However, even the finite lattice system has some interesting gap structure at $E = 0$ which we now discuss (see Fig. 5). Any finite size square lattice of dimensions ($L \times L$) shows a number of bands dispersing linearly from $E = 0$. This number and the slope increases in an interesting fashion, which can be guessed from our discussions on the finite size polygons in magnetic field. Note that a $L \times L$ square ring has $(L - 1)^2\alpha$ flux passing through it. Substituting $N = 4L - 4$, $M = N/4$ in Eqn. 3, we find the low energy dispersion of the form,

$$= -2t \cos\left(\frac{2\pi}{N}((L - 1) + (L - 1)^2\alpha)\right) \quad (4)$$

$$\approx (L - 1)\pi\alpha \quad (5)$$

Now a square lattice of $L \times L$ can contain states on concentric square rings of dimensions $2, 4, \dots, L$, where the

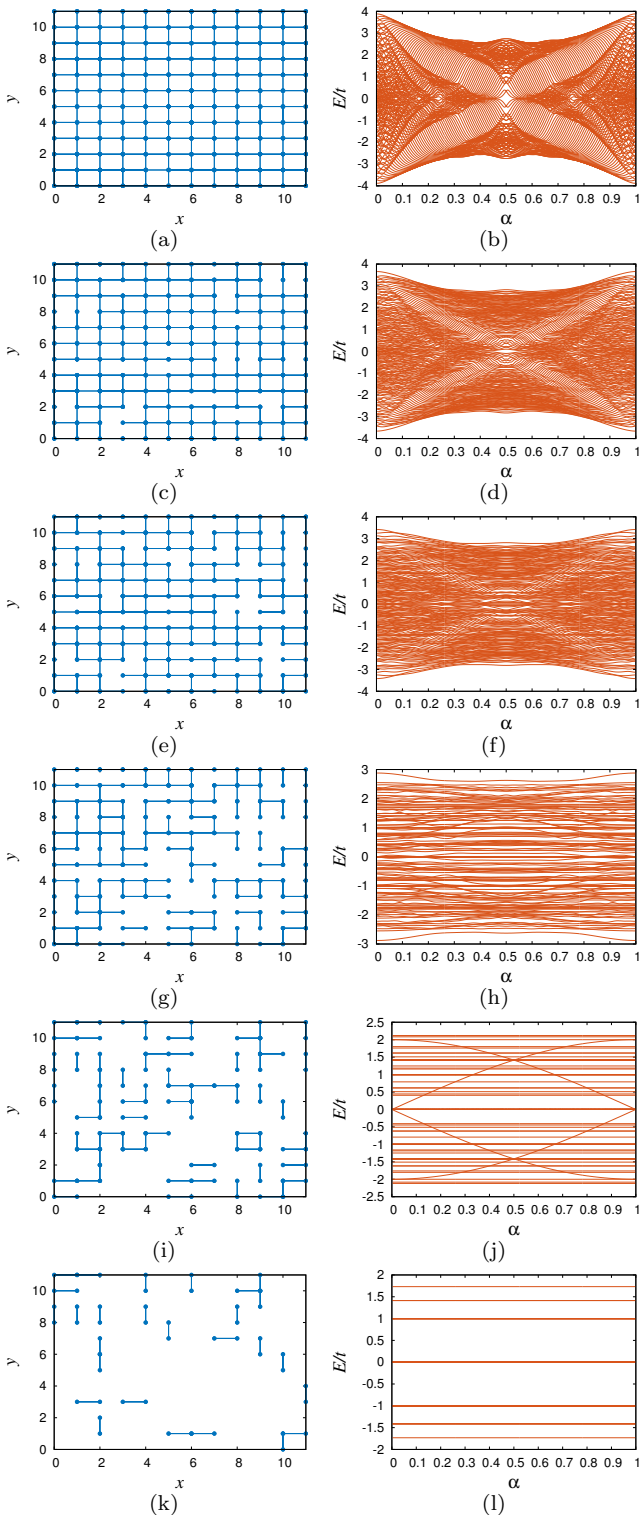


Fig. 4. (Color online) The representative lattices of 12×12 size at different values of p_b and their energy dispersion as a function of the magnetic flux α . The lattices shown in (a) belongs to $p_b = 1$. For (c) $p_b = 0.9$, (e) $p_b = 0.75$, (g) $p_b = 0.50$, (i) $p_b = 0.25$ and (k) $p_b = 0.1$. The corresponding dispersion as a function of α is shown in (b),(d),(f),(h),(j) and (k) respectively. (b) is the corresponding Hofstadter butterfly for a finite 12×12 system. While the increasing disorder destroys the butterfly pattern, one finds non-varying lines present in the dispersion. In (j) one finds only two bands dispersing. While in (l) one finds no dispersing bands.

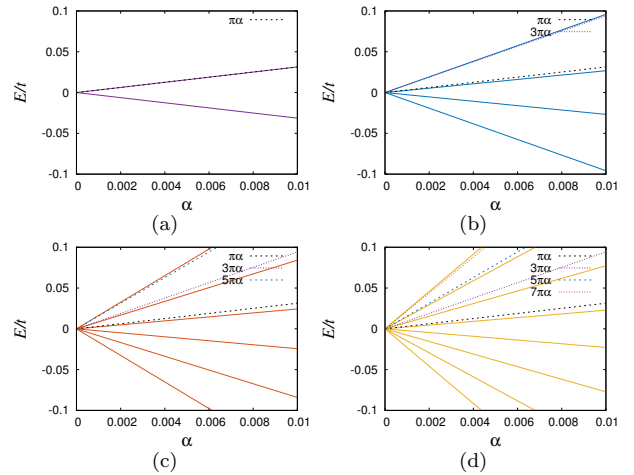


Fig. 5. (Color online) Band dispersion for square lattices with open periodic condition for lattices of size $L \times L$ for (a) 2×2 (b) 4×4 (c) 6×6 and (d) 8×8 for α and E close to zero. The slope of dispersion approximately follows the slope of $\pi(L-1)\alpha$

states on this rings have small α dispersion as $\pi\alpha, 3\pi\alpha \dots (L-1)\pi\alpha$ near $E = 0$. This can be clearly seen from Fig. 5. As is expected the states indeed lie predominantly on the concentric rings.

3.0.4 $p_b \gg p_c$

We now look at the effect of the low bond disorder on the finite size Hofstadter butterfly. We focus on the band gap structure at $E = 0$. We see from Fig.6, a pure 4×4 and 12×12 ((a) and (b)) lattice size has a set of gapless points and large band gaps at some other values of α . Increasing disorder, opens up gaps at the gapless points and reduces otherwise large band gaps. This, in some sense, is the usual effect of any disorder i.e. spreading of the DOS . It is also reasonable to see that this effect increases with increasing disorder. This is more clear from the inset in the Fig.6 where the variance of the gap is plotted. We also note that the amount of gap opened up at $\alpha = 0$ is much smaller than other gap-less points.

To further understand the effect of bond percolation disorder, we study the Inverse Participation Ratio (IPR) of the different wavefunctions. IPR for a unit normalized wavefunction $|\psi\rangle$ expandable in site basis as,

$$|\psi\rangle = \sum_i \psi_i |i\rangle \quad (6)$$

is given by,

$$IPR = \sum_i |\psi_i|^4 \quad (7)$$

This value estimates the spread of a wavefunction in real space. For a delocalized wavefunction spread uniformly over area A , $IPR \propto 1/A$, and will decrease with increasing area. If a wavefunction is localized over some few sites, then $IPR \propto 0.1 - 1$ and doesn't change significantly with increasing size of the system. This diagnostic therefore

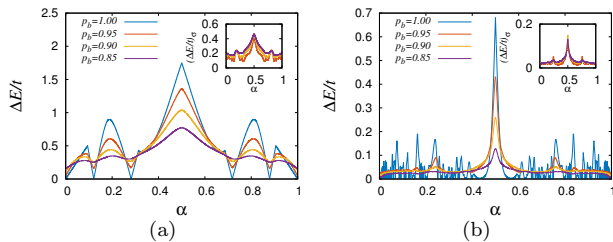


Fig. 6. (Color online) The band gap at $E = 0$ for four values of $p_b = 1.0, 0.95, 0.90$ and 0.85 as a function of α for a (a) 4×4 lattice and (b) 12×12 lattice. For the later three values of p_b , averages are being plotted over 400 configurations. The blue line is for the pure system, and has many gapless points and large band gaps including one at $\alpha = 0.5$. Increasing the disorder, opens up the gap at gapless points and reduces the magnitude of the larger gaps from the pure system. The lower the value of p_b , the effect is larger. In the Inset, the variance ($\equiv (\Delta E/t)_\sigma$) for the later three values of p_b are plotted. It shows the variance $\Delta E/t$ increase with decrease in p_b . All these are consistent with our understanding that generic weak disorder spreads out the DOS and open up gaps at the gapless points.

provides a scope to demarcate localized and delocalized states. To estimate the effect on IPR, we consider 400 configurations of the lattice at a given p_b . For each configuration we diagonalize the Hamiltonian and innumerate the energy eigenvalues as $n = 1 \dots L^2$. For each value of n we average over the eigenvalues to find the average energy, and their IPRs to find the average IPR. This gives us the average IPR of the full system as a function of energy and is shown in Fig. 7. As the p_b is reduced, IPR at certain values of E becomes very large. Interestingly the values are at $\pm t$, $\pm\sqrt{2}t$ and $\pm\sqrt{3}t$. These correspond to clusters of small sites mentioned before. The corresponding IPRs for these is $1, 1/2$ and $1/3$. As p_b is decreased further some of these peaks vanish, and now only the central peak remains. Also peaks at other values correspond to the solutions for a open tight binding chain. For a n -site chain the dispersion is given by $-2t \cos k$, where $k \in \frac{m\pi}{n+1}$, where $m \in (1, 2, \dots, n)$. For example, a 4-site open chain has eigenvalues at $\pm 2 \cos(\frac{\pi}{5}) (\sim \pm 0.62)$ and $\pm 2 \cos(\frac{2\pi}{5}) (\sim \pm 1.62)$ which can also be clearly seen in Fig. 7 (a).

In Fig. 7(b) we look at relatively smaller values of p_b and look at the effect of increasing the system size. The variation of IPR signifies whether the system is comprised of localized or delocalized states. For example at $p_b = 1.0$ one finds that IPR is quite low ($\sim 5 \times 10^{-3}$) and reduces with increasing system size. Decreasing p_b one notices a strong peak appears at $E = 0$, implying appearance of localized states. However, one notices that decreasing p_b more high IPR peaks start to appear at distinct energy values as discussed in detail above. However, interestingly the average IPR of the system increases, and the value for 30×30 starts to overlap with 24×24 , implying localization overall in the full spectrum. This feature becomes quite prominent at $p_b \lesssim 0.65$. Note that the average IPR is about 0.025 at $p_b = 0.60$ signaling that the wavefunction resides only on a average of 40 sites, in otherwise a lat-

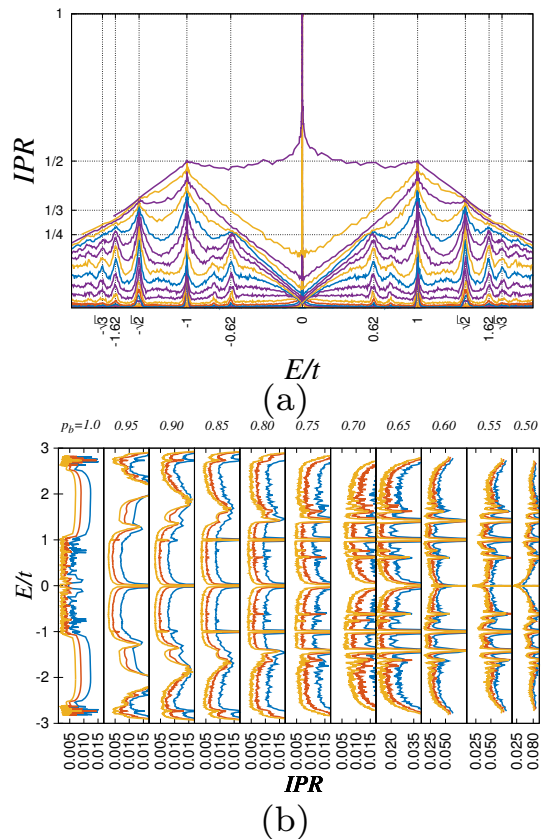


Fig. 7. (Color online) Variation of IPR as a function of bond probability. (a) IPR is shown for a 30×30 lattice for p_b starting from 1.0 (bottom-most) to 0.05 (top-most) in intervals of 0.05. One notices appearance of peaks at specific values of E/t which goes away with reducing p_b . (see text) (b) IPR for system sizes 18×18 (blue), 24×24 (orange) and 30×30 (yellow) compared to each other at $\alpha = 1/4$ when averaged over 400 configurations. At $p_b = 1.0$ the IPR is quite small ($\sim 5 \times 10^{-3}$) and reduces with increasing system size. Decreasing p_b one notices a strong peak appears at $E = 0$, implying appearance of localized states. However, one notices that decreasing p_b more high IPR peaks start to appear at distinct energy values. Also the average IPR of the system increases for a 30×30 lattice and overlaps with the case of 24×24 , implying overall localization in the spectrum. This feature becomes prominent for $p_b \lesssim 0.65$. Error bars are not shown for clarity of figure.

tice of 900 sites. This signals the wavefunctions have got localized much before the classical percolation threshold is reached. This will be investigated more clearly through calculations of the transport in the next section.

4 Effect on Chern numbers and Transport

Hofstadter Model, apart from structure of the eigenspectrum, also hosts interesting structure of the topological invariants [17, 18, 59]. It will be interesting to understand the effect of disorder on such topological invariants. This therefore requires calculation of Chern numbers. Note that in presence of disorder, the system no longer contains

translational symmetry and therefore a momentum integral over the Brillouin zone will not suffice to calculate the Chern number. We therefore calculate the Chern numbers using the method outlined in [54]. This essential numerical technique is motivated from the fact that Chern number can also be calculated from an integral over the twisted boundary conditions. For completeness we include briefly some of the definitions and a brief discussion about the method following [54].

For a 2D lattice comprising of $N = L \times L$ unit cells, the single particle wavefunctions can satisfy the following boundary conditions given by $\phi_\theta(x + L, y) = e^{i\theta_x} \phi_\theta(x, y)$ and $\phi_\theta(x, y + L) = e^{i\theta_y} \phi_\theta(x, y)$, where $\theta = (\theta_x, \theta_y)$ such that $0 \leq \theta_x, \theta_y \leq 2\pi$. For a given filling, we can have M states occupied. Let the many body wavefunction of these M states be written as Ψ_θ . Then the Chern number of the ground state is given by

$$C = \frac{1}{2\pi i} \int_{T_\theta} d\theta \langle \nabla_\theta \Psi_\theta | \times | \nabla_\theta \Psi_\theta \rangle \quad (8)$$

where T_θ denotes the allowed (θ_x, θ_y) values [60].

Note that since in defining Ψ we have taken into consideration all the filled states, C here is the sum of the Chern numbers of individual bands below the chemical potential. Hence the quantity evaluated can be interpreted as σ_{xy} in units of e^2/h .

The calculation of σ_{xy} can be directly done using Lehmann representation of the Kubo formula [61]. However finding the Chern number of each band requires numerical diagonalization of a system many number of times [30]. The recently developed coupling matrix approach allows for a much simpler and numerically inexpensive method [54]. The idea is to convert the integral over T_θ into an integral over a path in momentum space. This integral then can be solved as a product of matrices whose components are determined by the inner product of some wavefunctions which were determined only by the system under periodic boundary conditions. The essential simplifying step is to do away with the necessity of diagonalizing the system at different values of boundary conditions. This approach can also take into consideration the effect of real space disorder in a natural way.

Now we present the results of our calculations. In Fig.8 we show the variation of σ_{xy} with bond occupation probability p_b for $p/q = 1/4$. The filling is kept constant at $1/4$ and for each configuration chemical potential is self consistently evaluated. The lattice size is systematically increased from 12×12 to 24×24 in difference of 4 sites per side. We find that increasing lattice size makes the transition sharper and clearly the conductance goes to zero much before p_c which occurs at $p_b = 0.5$. The transition seems to occur close to $p_b \approx 0.65$, which was also tentatively the value seen from IPR results in previous section.

In Fig.9 we show the variation of σ_{xy} with bond occupation probability p_b for $p/q = 1/16$ for different fillings. We find that with increasing filling the Chern insulator plateau remains stable only for lower strength of bond disorder. Note that with increasing filling from $1/16$ to $7/16$ we moved from bottom of the spectrum to band center.

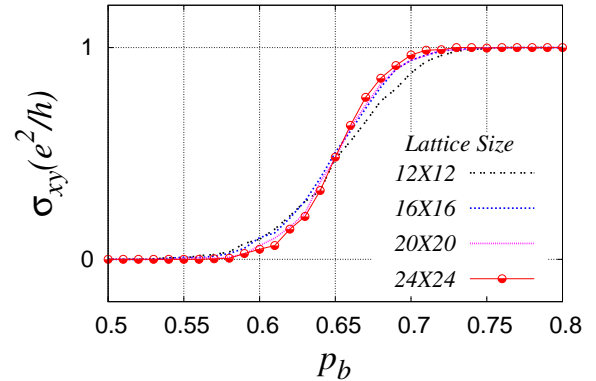


Fig. 8. (Color online) Plot of σ_{xy} with bond occupation probability p_b at $p/q = 1/4$ for different lattice sizes. The filling is kept constant at $1/4$ and the lattice size is increased from 12×12 to 24×24 . The red line with moon points is for the lattice size of 24×24 . The results are averaged over 400 disorder configurations. With increasing lattice size we find the transition becoming sharper around $p_b \approx 0.65$. The *standard error* of the mean is of the order of the point size or lower and hence has not been shown above.

This resembles what was found for the Anderson disorder in earlier studies [30].

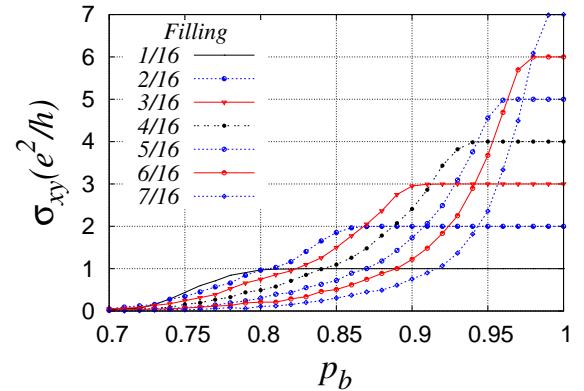


Fig. 9. (Color Online) σ_{xy} with bond occupation probability p_b for $p/q = 1/16$ for different fillings. The lattice size is 32×32 . The results are averaged over 400 disorder configurations. In the clean limit ($p_b = 1$) σ_{xy} for fillings $n/16$ is $n \frac{e^2}{h}$ where ($n \in 1, \dots, 7$). With increasing filling one moves from the bottom of the full spectrum to the center. The Chern insulator plateaus are less stable to bond disorder as one moves closer to band center.

To understand the underlying mechanism for this, one first realizes that the physics of the Hofstadter problem is different from that of the continuum 2D model. Unlike the continuum, σ_{xy} can be negative in the lattice setting [59]. This is because the bands here may carry negative Chern numbers. For an even q a negative Chern number band of Chern number $-2(q-1)$ lies at the band center. With in-

creasing onsite disorder it has been argued that this central band mixes with the other bands hence explaining why the bands close to band center are the first ones to show transition to normal insulator [30]. We infer that the similar considerations indeed apply in this limit of bond percolation problem.

Also there is a lot of interest in understanding the physics in the limit of *zero* magnetic field. We expect that with weakening magnetic field, the amount of bond percolation disorder required for Anderson insulating transition will decrease i.e. p_q will slowly approach a larger value. This can be expected from Fig. 8 and Fig. 9. The magnetic flux is kept high ($p/q = 1/4$) in Fig. 8 and the transition occurs at $p_b \approx 0.65$. While in Fig. 9 the magnetic flux is kept low ($p/q = 1/16$), and the transitions for all values of filling occurs at $p_b > 0.65$. This suggests that with further decrease in magnetic field, one might expect higher values of p_b (lower number of bonds removed) where the transition will occur. The exact form of this variation and its filling dependence would be interesting to investigate.

5 Summary and Future Directions

To summarize, we have studied the effect of the bond percolation disorder on the Hofstadter bands which are formed when a perpendicular magnetic field is applied to a square lattice. We have looked at the evolution of the Hofstadter butterfly as the bond percolation is increased. We find that at low values of p_b , unlike the Anderson disorder, the eigenspectrum does-not disperse with the magnetic field. This we attribute to the open clusters of sites which do not enclose any magnetic field. With slight increase in p_b we find few dispersing states which are due to disconnected rings. The dispersion of these are compared with finite size ring structures. At large values of p_b we find the bond percolation spreads out energy eigenvalues and the gapless points get opened up. We also analyze the IPR of the wavefunctions as a function of p_b , and have looked at the effect of this disorder on band gaps and states close to $E = 0$. To understand some of the features of our results we discussed properties of finite size rings and clusters.

Next we investigated the effect of disorder on the Chern bands, and found that they undergo direct transition to the normal insulator state with increasing bond percolation disorder. This happens at a bond occupation probability p_b higher than the classical percolation threshold. We also find that the bands at the band bottom are more stable to disorder than the band center. The calculations were performed using a recently developed method of calculating Chern numbers using coupling matrix approach [54]. These results seem to be in accordance with the insights found from the diagonal Anderson disorder problem [30].

We now mention some of the future directions. In our study, we have looked at two aspects of the physics of bond percolation on square lattices when kept in presence of uniform magnetic field. One, the effect on the energy

dispersion, which leads to the effective ‘‘killing’’ of the Hofstadter butterfly. And two, effect on transverse conductivity σ_{xy} . It will be interesting to look at the magnetic oscillations in this system for a fixed density of particles. Magnetization (M) is determined by the change of the energy dispersion of the system as a function of magnetic field $M = -\frac{\partial E}{\partial \alpha}$ [62]. If the energy spectrum does not disperse with magnetic field (α), as is the case when $p_b \ll p_c$, then this quantity will be identically *zero*. Therefore absence of oscillations due to increasing bond-percolation is a signature of reaching the limit of high percolation disorder. However, the exact form of this change and the variation with p_b may be interesting to understand.

Further, while we study the effect of bond percolation on the σ_{xy} , it might be interesting to correlate this with the effect on σ_{xx} . It will be intriguing to understand if the two-parameter scaling theory, as has been tested for other disorder problems in quantum Hall physics [32], is also applicable to the bond percolation disorder. There are other interesting parallels between the Anderson transition and percolation transition which would be worth pursuing. It was shown in [63], that both percolation and Anderson transition have a characteristic exponent by which the radius of a wavepacket spreads with time. It might be interesting to study these exponents in presence of a magnetic field and investigate the transitions from the Hall state to an Anderson insulator state. In [64] existence of weaker Anderson transitions was shown for diagonal disorder in $2D$. It might also be interesting to realize this physics in case of percolation disorder and study its interplay with the effects of a perpendicular magnetic field.

Financial support from CSIR, India is gratefully acknowledged. AA is grateful to Vijay B. Shenoy for suggestions, discussions and computational resources. AA also thanks Sambudha Sanyal, Jayantha P. Vyasanakere and Ajit C. Balram for discussions and for comments on the manuscript.

References

1. Patrick A. Lee and T. V. Ramakrishnan. Disordered electronic systems. *Rev. Mod. Phys.*, 57:287–337, Apr 1985.
2. B Kramer and A MacKinnon. Localization: theory and experiment. *Reports on Progress in Physics*, 56(12):1469, 1993.
3. Martin Janssen. Statistics and scaling in disordered mesoscopic electron systems. *Physics Reports*, 295(12):1 – 91, 1998.
4. Ferdinand Evers and Alexander D. Mirlin. Anderson transitions. *Rev. Mod. Phys.*, 80:1355–1417, Oct 2008.
5. Elihu Abrahams, Sergey V. Kravchenko, and Myriam P. Sarachik. Metallic behavior and related phenomena in two dimensions. *Rev. Mod. Phys.*, 73:251–266, Mar 2001.
6. P. W. Anderson. Absence of diffusion in certain random lattices. *Phys. Rev.*, 109:1492–1505, Mar 1958.
7. Horst L. Stormer, Daniel C. Tsui, and Arthur C. Gosard. The fractional quantum hall effect. *Rev. Mod. Phys.*, 71:S298–S305, Mar 1999.
8. K. S. Novoselov. Nobel lecture: Graphene: Materials in the flatland*. *Rev. Mod. Phys.*, 83:837–849, Aug 2011.

9. S. Das Sarma, Shaffique Adam, E. H. Hwang, and Enrico Rossi. Electronic transport in two-dimensional graphene. *Rev. Mod. Phys.*, 83:407–470, May 2011.
10. M. Z. Hasan and C. L. Kane. *Colloquium* : Topological insulators. *Rev. Mod. Phys.*, 82:3045–3067, Nov 2010.
11. K. v. Klitzing, G. Dorda, and M. Pepper. New method for high-accuracy determination of the fine-structure constant based on quantized hall resistance. *Phys. Rev. Lett.*, 45:494–497, Aug 1980.
12. Douglas R. Hofstadter. Energy levels and wave functions of bloch electrons in rational and irrational magnetic fields. *Phys. Rev. B*, 14:2239–2249, Sep 1976.
13. M. Aidelsburger, M. Atala, M. Lohse, J. T. Barreiro, B. Paredes, and I. Bloch. Realization of the hofstadter hamiltonian with ultracold atoms in optical lattices. *Phys. Rev. Lett.*, 111:185301, Oct 2013.
14. Hirokazu Miyake, Georgios A. Siviloglou, Colin J. Kennedy, William Cody Burton, and Wolfgang Ketterle. Realizing the harper hamiltonian with laser-assisted tunneling in optical lattices. *Phys. Rev. Lett.*, 111:185302, Oct 2013.
15. B. Hunt, J. D. Sanchez-Yamagishi, A. F. Young, M. Yankowitz, B. J. LeRoy, K. Watanabe, T. Taniguchi, P. Moon, M. Koshino, P. Jarillo-Herrero, and R. C. Ashoori. Massive dirac fermions and hofstadter butterfly in a van der waals heterostructure. *Science*, 340(6139):1427–1430, 2013.
16. G. L. Yu, R. V. Gorbachev, J. S. Tu, A. V. Kretinin, Y. Cao, R. Jalil, F. Withers, L. A. Ponomarenko, B. A. Piot, M. Potemski, D. C. Elias, X. Chen, K. Watanabe, T. Taniguchi, I. V. Grigorieva, K. S. Novoselov, V. I. Fal'ko, A. K. Geim, and A. Mishchenko. Hierarchy of hofstadter states and replica quantum hall ferromagnetism in graphene superlattices. *Nat Phys*, 10(7):525–529, Jul 2014. Article.
17. D. J. Thouless, M. Kohmoto, M. P. Nightingale, and M. den Nijs. Quantized hall conductance in a two-dimensional periodic potential. *Phys. Rev. Lett.*, 49:405–408, Aug 1982.
18. D. Osadchy and J. E. Avron. Hofstadter butterfly as quantum phase diagram. *Journal of Mathematical Physics*, 42(12):5665–5671, 2001.
19. J T Chalker and P D Coddington. Percolation, quantum tunnelling and the integer hall effect. *Journal of Physics C: Solid State Physics*, 21(14):2665, 1988.
20. P. Cain, R. A. Römer, M. Schreiber, and M. E. Raikh. Integer quantum hall transition in the presence of a long-range-correlated quenched disorder. *Phys. Rev. B*, 64:235326, Nov 2001.
21. A. G. Galstyan and M. E. Raikh. Localization and conductance fluctuations in the integer quantum hall effect: Real-space renormalization-group approach. *Phys. Rev. B*, 56:1422–1429, Jul 1997.
22. B. Kramer, T. Ohtsuki, and S. Kettemann. Random network models and quantum phase transitions in two dimensions. *Physics Reports*, 417(56):211 – 342, 2005.
23. Bodo Huckestein. Scaling theory of the integer quantum hall effect. *Rev. Mod. Phys.*, 67:357–396, Apr 1995.
24. M. Ortuño, A. M. Somoza, V. V. Mkhitarian, and M. E. Raikh. Phase diagram of the weak-magnetic-field quantum hall transition quantified from classical percolation. *Phys. Rev. B*, 84:165314, Oct 2011.
25. Valery Timofeevich Dolgoplov. Integer quantum hall effect and related phenomena. *Physics-Uspokhi*, 57(2):105, 2014.
26. E. Abrahams, P. W. Anderson, D. C. Licciardello, and T. V. Ramakrishnan. Scaling theory of localization: Absence of quantum diffusion in two dimensions. *Phys. Rev. Lett.*, 42:673–676, Mar 1979.
27. D.E. Khmel'nitskii. Quantum hall effect and additional oscillations of conductivity in weak magnetic fields. *Physics Letters A*, 106(4):182 – 183, 1984.
28. R. B. Laughlin. Levitation of extended-state bands in a strong magnetic field. *Phys. Rev. Lett.*, 52:2304–2304, Jun 1984.
29. Kun Yang and R. N. Bhatt. Floating of extended states and localization transition in a weak magnetic field. *Phys. Rev. Lett.*, 76:1316–1319, Feb 1996.
30. D. N. Sheng and Z. Y. Weng. Disappearance of integer quantum hall effect. *Phys. Rev. Lett.*, 78:318–321, Jan 1997.
31. A. M. M. Pruisken. Dilute instanton gas as the precursor to the integral quantum hall effect. *Phys. Rev. B*, 32:2636–2639, Aug 1985.
32. D. N. Sheng and Z. Y. Weng. New universality of the metal-insulator transition in an integer quantum hall effect system. *Phys. Rev. Lett.*, 80:580–583, Jan 1998.
33. D. N. Sheng and Z. Y. Weng. Phase diagram of the integer quantum hall effect. *Phys. Rev. B*, 62:15363–15366, Dec 2000.
34. Scott Kirkpatrick. Percolation and conduction. *Rev. Mod. Phys.*, 45:574–588, Oct 1973.
35. A Mookerjee, T Saha-Dasgupta, and I Dasgupta. Quantum transmittance through random media. *Quantum and Semi-classical Percolation and Breakdown in Disordered Solids*, 762:83, 2009.
36. Th. Koslowski and W. von Niessen. Mobility edges for the quantum percolation problem in two and three dimensions. *Phys. Rev. B*, 42:10342–10347, Dec 1990.
37. M Fhokrul Islam and Hisao Nakanishi. Localization-delocalization transition in a two-dimensional quantum percolation model. *Phys. Rev. E*, 77:061109, Jun 2008.
38. Longyan Gong and Peiqing Tong. Localization-delocalization transitions in a two-dimensional quantum percolation model: von neumann entropy studies. *Phys. Rev. B*, 80:174205, Nov 2009.
39. S. Brianna Dillon and Hisao Nakanishi. Localization phase diagram of two-dimensional quantum percolation. *The European Physical Journal B*, 87(12):1–9, 2014.
40. Dietrich Stauffer and Amnon Aharony. *Introduction to percolation theory*. Taylor and Francis, 1991.
41. M. B. Isichenko. Percolation, statistical topography, and transport in random media. *Rev. Mod. Phys.*, 64:961–1043, Oct 1992.
42. C. M. Soukoulis and Gary S. Grest. Localization in two-dimensional quantum percolation. *Phys. Rev. B*, 44:4685–4688, Sep 1991.
43. T. Odagaki, M. Lax, and A. Puri. Hopping conduction in the d -dimensional lattice bond-percolation problem. *Phys. Rev. B*, 28:2755–2765, Sep 1983.
44. Raghu Raghavan and Daniel C. Mattis. Eigenfunction localization in dilute lattices of various dimensionalities. *Phys. Rev. B*, 23:4791–4793, May 1981.
45. Yonathan Shapir, Amnon Aharony, and A. Brooks Harris. Localization and quantum percolation. *Phys. Rev. Lett.*, 49:486–489, Aug 1982.

46. J P G Taylor and A MacKinnon. A study of the two-dimensional bond quantum percolation model. *Journal of Physics: Condensed Matter*, 1(49):9963, 1989.
47. Daniel Schmidtke, Abdellah Khodja, and Jochen Gemmer. Transport in tight-binding bond percolation models. *Phys. Rev. E*, 90:032127, Sep 2014.
48. S. Sanyal, K. Damle, and O. I. Motrunich. Vacancy-induced low-energy states in undoped graphene. *ArXiv e-prints*, February 2016.
49. V. Häfner, J. Schindler, N. Weik, T. Mayer, S. Balakrishnan, R. Narayanan, S. Bera, and F. Evers. Density of states in graphene with vacancies: Midgap power law and frozen multifractality. *Phys. Rev. Lett.*, 113:186802, Oct 2014.
50. P. M. Ostrovsky, I. V. Protopopov, E. J. König, I. V. Gornyi, A. D. Mirlin, and M. A. Skvortsov. Density of states in a two-dimensional chiral metal with vacancies. *Phys. Rev. Lett.*, 113:186803, Oct 2014.
51. Lin Zhu and Xu Wang. Singularity of density of states induced by random bond disorder in graphene. *Physics Letters A*, pages –, 2016.
52. Wen-Sheng Liu and XL Lei. Integer quantum hall transitions in the presence of off-diagonal disorder. *Journal of Physics: Condensed Matter*, 15(17):2693, 2003.
53. Yigal Meir, Amnon Aharony, and A. Brooks Harris. Quantum percolation in magnetic fields. *Phys. Rev. Lett.*, 56:976–979, Mar 1986.
54. Zhang Yi-Fu, Yang Yun-You, Ju Yan, Sheng Li, Shen Rui, Sheng Dong-Ning, and Xing Ding-Yu. Coupling-matrix approach to the chern number calculation in disordered systems. *Chinese Physics B*, 22(11):117312, 2013.
55. James G. Analytis, Stephen J. Blundell, and Arzhang Ardavan. Landau levels, molecular orbitals, and the hofstadter butterfly in finite systems. *American Journal of Physics*, 72(5):613–618, 2004.
56. N. Weik, J. Schindler, S. Bera, G. C. Solomon, and F. Evers. Graphene with vacancies: supernumerary zero modes. *ArXiv e-prints*, March 2016.
57. Peter Markos. Numerical analysis of the anderson localization. *Acta Physica Slovaca*, 56(5):561 – 685, 2006.
58. Timothy A. L. Ziman. Localization with off-diagonal disorder: A qualitative theory. *Phys. Rev. B*, 26:7066–7069, Dec 1982.
59. Eduardo Fradkin. *Field theories of condensed matter systems*, volume 7. Addison-Wesley Redwood City, 1991.
60. Qian Niu, D. J. Thouless, and Yong-Shi Wu. Quantized hall conductance as a topological invariant. *Phys. Rev. B*, 31:3372–3377, Mar 1985.
61. Paramita Dutta, Santanu K. Maiti, and S. N. Karmakar. Integer quantum hall effect in a lattice model revisited: Kubo formalism. *Journal of Applied Physics*, 112(4):–, 2012.
62. James G. Analytis, Stephen J. Blundell, and Arzhang Ardavan. Magnetic oscillations, disorder and the hofstadter butterfly in finite systems. *Synthetic Metals*, 154(13):265 – 268, 2005. Proceedings of the International Conference on Science and Technology of Synthetic MetalsPart {III}.
63. Atsushi Kaneko, Daisuke Uema, and Tomi Ohtsuki. Quantum percolation and the anderson transition. *Journal of the Physical Society of Japan*, 72(Suppl. A):141–142, 2003.
64. Nigel Goldenfeld and Roger Haydock. Phase diagram for anderson disorder: Beyond single-parameter scaling. *Phys. Rev. B*, 73:045118, Jan 2006.